Green Chemistry

Accepted Manuscript

This article can be cited before page numbers have been issued, to do this please use: W. Li, G. Fan, L. Yang and F. Li, *Green Chem.*, 2017, DOI: 10.1039/C7GC01387F.

ROYAL SOCIETY OF CHEMISTRY

rsc.li/green-chem

View Article Online
DOI: 10.1039/C7GC01387F

Journal Name

ARTICLE

Highly efficient synchronized production of phenol and 2,5-dimethylfuran through a bimetallic Ni-Cu catalyzed dehydrogenation-hydrogenation coupling process without external hydrogen and oxygen supply

Wei Li,[a,b] Guoli Fan,[a] Lan Yang [a] and Feng Li*[a]

2,5-Dimethylfuran (DMF) and phenol are considered as one of the new-fashioned liquid transportation biofuels and the most key structural motifs for industrial chemicals, respectively. Herein, a highly efficient vapor-phase dehydrogenation-hydrogenation coupling process over bimetallic Ni-Cu alloy nanocatalysts was established for the synchronized production of phenol and DMF with unprecedentedly high yields (>97%) from two cyclohexanol (CHL) and biomass-derived 5-hydroxymethylfurfural (HMF) substrates, without external hydrogen and oxygen supply. Systematic characterizations and catalytic experiments revealed that the production of phenol went through a consecutive triple-dehydrogenation process from CHL, while HMF was simultaneously hydrogenated into DMF using active hydrogen species generated from the dehydrogenation. The bimetallic Ni-Cu alloy nanostructures derived from Ni-Cu-Al layered double hydroxide precursors and strong metal-support interactions play important roles in governing the present coupling process. An appropriate Ni-Cu alloy nanostructure could greatly facilitate the dehydrogenative aromatization of CHL, thus significantly improving the selectivities to both phenol and DMF. Such an unparalleledly efficient, eco-friendly and versatile coupling process for the synchronized production of various substituted phenols and DMF makes it practical promising for large-scale industrial applications in terms of green chemistry and sustainable development.

Received 00th January 20xx,
Accepted 00th January 20xx

DOI: 10.1039/x0xx00000x

www.rsc.org/

Introduction

With the growing shortage of fossil resources and the increase in greenhouse gas emissions, the associated energy crisis and environmental pollution are gaining increasing attention.[1] In recent years, considerable interest has been oriented towards the development of sustainable resources for bulk chemicals and energy production in both academic and industrial communities. Especially, the conversion from renewable raw biomass resources into high-quality liquid biofuels and high value-added chemicals is undoubtedly the most attractive.[2,3] With the development of transportation and economics involved, natural carbohydrates are considered as potential candidates for the synthesis of renewable liquid biofuels because they can provide the largest carbon source for transportation fuels and important chemicals.[4] In this regard, biomass-derived 5-hydroxymethyl-furfural (HMF) is perceived as a versatile key platform compound in the biomass conversion for a broad array of biofuels through reductive upgrading, and efforts to use such building blocks have been going on for quite some while.[5] In particular, 2,5-dimethylfuran (DMF), which can be produced by the selective hydrodeoxygenation of HMF, shows great potential as a liquid biofuel additive, thanks to the unique properties including low boiling point (92–94 °C), high research octane number (111), high energy density (31.5 MJ/L) and low water solubility.[6]

Presently, the conversion of HMF into DMF using molecular hydrogen has been extensively explored over various metal and bimetallic catalysts.[7] Specially, bimetallic catalysts (e.g. Cu-Ru,[3a] Pt-Co[7f-h]) usually presents higher selectivity to DMF than monometallic analogues. Even so, in some cases, DMF selectivities are poor as a consequence of the occurrence of further ring-opened and ring-hydrogenated reactions. Although noble metal catalysts show good catalytic performance, some drawbacks, such as easy deactivation, limit their practical applications. Therefore, for the energy

[a] State Key Laboratory of Chemical Resource Engineering, Beijing Advanced Innovation Center for Soft Matter Science and Engineering, Beijing University of Chemical Technology, Beijing 100029, China.
E-mail: lifeng@mail.buct.edu.cn; Fax: +8610-64425385; Tel: +86-10-64451226
[b] SINOPEC Beijing Research Institute of Chemical industry Yanshan Branch, Beijing 102500, China.
†Electronic supplementary information (ESI) available. See DOI: 10.1039/x0xx00000x

View Article Online
DOI: 10.1039/C7GC01387F

conversion, developing heterogeneous noble metal-free catalysts is highly desirable from both an economic and a sustainable development perspective. Conventionally, the hydrodeoxygenation of HMF always consumes external hydrogen. However, there are some drawbacks in the hydrogenation using molecular hydrogen, such as high hydrogen pressure, hydrogen flammability, and high costs of hydrogen transportation and storage. More recently, hydrogenations of HMF using formic acid or alcohols as hydrogen sources also have emerged.[6d,8] Despite the technical viability of these alternative hydrogen donors, the application of this strategy, however, meets great challenges due to several issues (e.g. the corrosiveness of formic acid, the use of large amounts of hydrogen donators as solvents).

On the other side, phenol and its derivatives as important precursors and core structural motifs of industrial chemicals are employed widely to manufacture polymers, dyes, agrochemicals, and pharmaceuticals.[9] Typically, phenol can be produced by a classical three-step cumene process involving the electrophilic aromatic substitution between benzene and propylene.[10] However, such widely employed commercial process also has several shortcomings including the involvement of explosive cumene hydroperoxide intermediate and the limitation in preparing *ortho*- or *para*-substituted derivatives due to the strong electronic directing effects associated with these reactions. Moreover, because of the high value of phenol, the preparation of cyclohexanol through cyclohexane oxidation has been explored,[11] instead of the phenol hydrogenation process. Recently, a newly-developed alternative process for the production of phenol, aerobic oxidative dehydrogenation of cyclohexanol (CHL) or cyclohexanone (CHN), has received increasing attention.[12] In this sense, the dehydrogenation of cyclohexanol to produce phenol is meaningful. Despite remarkable progress in this process, most of the existing studies were carried out by using external oxidizing reagents (e.g. molecular oxygen or air) and noble metal catalysts. Therefore, the direct production of phenol based on the dehydrogenation of CHL or CHN over heterogeneous non-noble-metal catalysts without the use of oxidizing reagents is still a challenge.

Over the past few years, some vapor-phase hydrogenation-dehydrogenation coupling processes to simultaneously produce hydrogenated and dehydrogenated products have been occasionally reported,[13] which highlights the idea of sustainable and economical production of chemicals.[14] As a typical example, the coupling in the combination of CHL dehydrogenation and furfural hydrogenation can produce 2-methylfuran or furfuryl alcohol and CHN.[15] Due to low efficiency of catalysts, in some cases, however, external hydrogen supply or cycle still is required to maintain the hydrogen transfer process, and the desired phenol are rarely produced. In this sense, designing highly efficient heterogeneous catalysts is quite crucial for the feasibility of the process.

In the present work, we for the first time report the synchronized production of phenol and DMF with high yields (> 97 %) through an unparalleledly efficient, eco-friendly and versatile vapor-phase coupling process between the CHL dehydrogenation and the HMF hydrogenation over bimetallic Ni-Cu alloy nanocatalysts without external hydrogen and oxygen supply, as shown in Scheme 1. Here, bimetallic Ni-Cu alloy nanocatalysts were prepared from Ni-Cu-Al layered double hydroxide (NiCuAl-LDH) precursors.[16] The reaction pathways and network were investigated. More intriguingly, due to the great difference in the boiling point of phenol and DMF (181.9 °C and 93.1 °C under 101.3 kPa, respectively), the

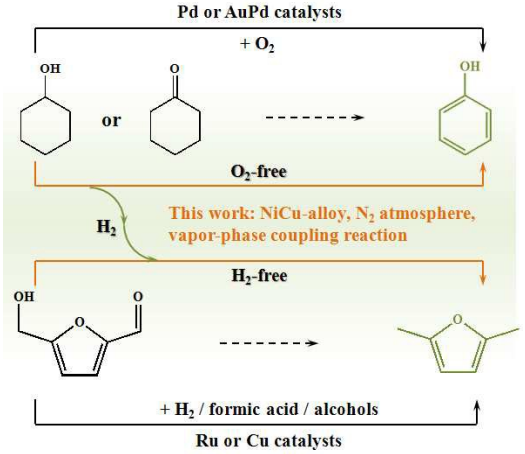

Scheme 1 The dehydrogenation-hydrogenation coupling process for the synchronized production of phenol and DMF, and the traditional synthetic procedures for phenol and DMF.

separation process of phenol and DMF would be easy, which may be of great importance for the large-scale industrial application of the coupling process. To the best of our knowledge, hitherto, the present developed bimetallic Ni-Cu alloy catalyzed vapor-phase dehydrogenation-hydrogenation coupling process for synchronized production of phenol and DMF with high yields starting from CHL and HMF substrates in the absence of hydrogen and oxygen has never been reported.

Results and discussion

Characterization of bimetallic Ni-Cu alloy nanocatalysts

Monometallic and bimetallic Ni-Cu catalysts (Ni_xCu_y) were prepared from NiCuAl-LDH precursors with different initial Ni:Cu molar ratios of *x*:*y* (see the ESI†). Other comparison samples with the identical metal loading to Ni_xCu_y catalysts were also prepared by the impregnation method.

Powder X-ray diffraction (XRD) patterns of different NiCuAl-LDH precursors show the characteristic diffractions of hydrotalcite-like materials (JCPDS 15-0087/37-0630) with well crystallinity (Fig. S1†). Fig. 1 shows the XRD patterns of reduced Ni_xCu_y samples under ambient conditions. Clearly, no diffraction peaks related to hydrotalcite-like materials can be found in reduced samples due to the topological transformation of LDH precursors. Monometallic Ni_3Cu_0 and Ni_0Cu_3 samples exhibit the characteristic (111) and (200) diffractions of

View Article Online
DOI: 10.1039/C7GC01387F

crystalline metallic nickel (JCPDS 04-0850) and metallic copper (JCPDS 04-0836) phases, respectively. In addition, the absence of crystalline Al_2O_3 reveals the existence of amorphous alumina phase as the support in samples. Interestingly, in the cases of bimetallic Ni_xCu_y samples, the (111) and (200) planes appear between those of metallic Ni and Cu peaks and their positions gradually shift to the higher values of 2 θ with the increasing Ni/Cu molar ratios from 1:2 to 2:1, strongly reflecting the formation of bimetallic Ni-Cu alloy phases.[17]

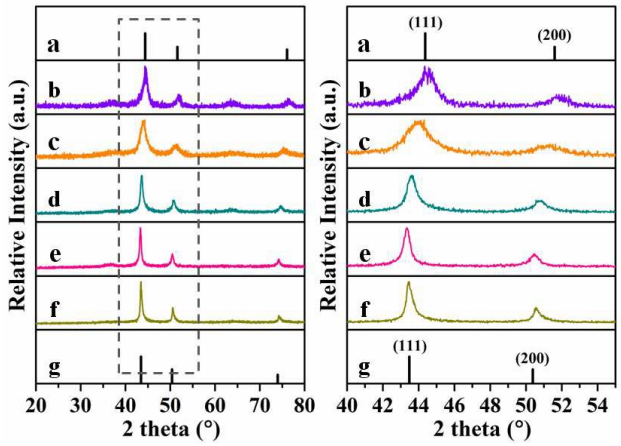

Fig. 1 XRD patterns of reduced Ni_xCu_y samples. (a) XRD standard card of Ni (JCPDS 04-0850), (b) Ni_3Cu_0, (c) Ni_2Cu_1, (d) $Ni_{1.5}Cu_{1.5}$, (e) Ni_1Cu_2, (f) Ni_0Cu_3, (g) XRD standard card of Cu (JCPDS 04-0836). Detailed XRD patterns (right) of different samples in the 2θ range of 40°–55°.

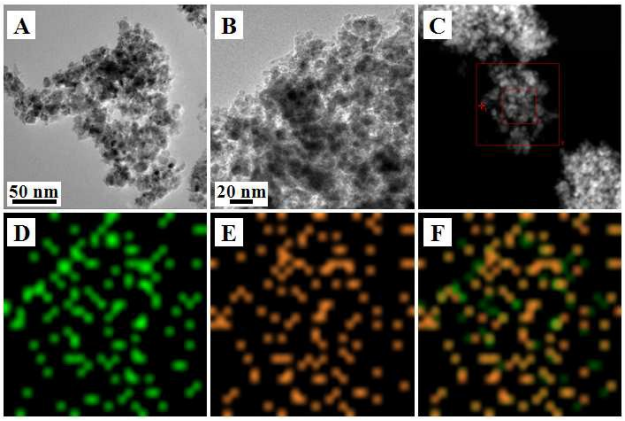

Fig. 2 HRTEM (A, B) and HAADF-STEM (C) images of the representative Ni_2Cu_1 sample; the EDS mappings of Ni (D), Cu (E) and the overlapping of Ni and Cu (F).

Further, high resolution transmission electron microscopy (HRTEM) and high-angle annular dark-field scanning TEM (HAADF-STEM) analysis of representative Ni_2Cu_1 sample (Fig. 2) depict that bimetallic Ni-Cu nanoparticles (NPs) can highly disperse on the surface. Elemental mapping analysis (Fig. 2D-3F) shows the homogeneous and similar distributions of Ni and Cu elements, further indicative of the formation of bimetallic Ni-Cu nanostructure. This result is also supported by the hydrogen temperature programmed reduction (H_2-TPR) results of calcined LDH samples (Fig. S2†). Notably, TPR profiles of all calcined NiCuAl-LDH samples show decreased reduction temperatures of both Ni and Cu species relative to calcined CuAl-LDH (278 °C for the reduction of Cu^{2+} species) and calcined NiAl-LDH (560 °C for the reduction of Ni^{2+} species) samples. Especially, the C-Ni_2Cu_1 sample (the precursor of Ni_2Cu_1 sample) shows the lowest reduction temperature, indicative of the improved reducibility of Ni and Cu species in the sample. The aforementioned results verify the presence of strong Ni-Cu interactions in calcined NiCuAl-LDH samples, thereby facilitating the formation of bimetallic Ni-Cu NPs. As shown in Table S1†, the specific surface area of samples ranging from about 74 to 90 m^2/g presents a gradual decrease with the decreasing Ni content, whereas the pore size shows an opposite trend.

Vapor-phase dehydrogenation-hydrogenation coupling process

Under nitrogen atmosphere, the vapor-phase coupling process goes through a consecutive two-part reaction pathway: CHL dehydrogenation to produce phenol; HMF hydrogenation to produce DMF using active hydrogen species released from the dehydrogenation part. Table 1 summarizes the catalytic reaction results over different Ni_xCu_y catalysts without external hydrogen and oxygen supply at 200 and 240 °C. It is noted that the yields of phenol and DMF decrease in the following order for catalysts: Ni_2Cu_1 > Ni_3Cu_0 > $Ni_{1.5}Cu_{1.5}$ > Ni_1Cu_2 >Ni_0Cu_3 (Table 1, entries 1-5). In particular, the highest yields of phenol (41%) and DMF (95%) are gained over the Ni_2Cu_1 at 200 °C. However, in the case of Ni_0Cu_3 catalyst, no phenol is formed and the main dehydrogenation product is CHN. Additionally, for Ni_3Cu_0, 2,5-dimethyltetrahydrofuran (DMTHF) product also can be detected as a consequence of the deep hydrogenation of the furan ring in DMF product.

The reaction results also indicate that when the reaction proceeds at 200 °C, high conversions of HMF (> 90%) can be achieved in each case, while the CHL conversion seems to be positively correlated with the Ni/Cu molar ratio in catalysts. When the reaction temperature is raised to 240 °C, the CHL conversion, along with the phenol yield, increases significantly. It is worth noting that a quite high phenol yield of 98% is achieved over the Ni_2Cu_1, higher than that over the Ni_3Cu_0 (Table 1, entries 6 and 7). Further decrease in the Ni/Cu molar ratio leads to the decrease in both CHL conversions and phenol yields (Table 1, entries 8 and 9). Only a low phenol yield of 8% is obtained over the Ni_0Cu_3 at 240 °C (Table 1, entry 10). It clearly demonstrates that Ni-rich catalysts exhibit superior catalytic activity to Cu-rich ones in the present coupling system; however, an appropriate incorporation of Cu into the Ni-Cu alloy structure can greatly facilitate the dehydrogenative aromatization of CHL, thereby improving the selectivities to both phenol and DMF. In addition, the coupling process also was conducted in the absence of any solvents. It is found that such process can be realized without any solvents (Table 1,

View Article Online
DOI: 10.1039/C7GC01387F

entry 11), despite a certain decrease in both conversions and product selectivities due to high concentrations of substrates.

Compared with Ni_3Cu_0, Ni_0Cu_3 and Ni_2Cu_1, three Ni/Al_2O_3, Cu/Al_2O_3 and $Ni\text{-}Cu/Al_2O_3$ comparison catalysts prepared by the impregnation method show much lower activities (Table 1, entries 12-14), along with lower conversions and phenol yields. In addition, lower yields of phenol and DMF are obtained over the physical mixture of Ni_3Cu_0 and Ni_0Cu_3 with the same Ni/Cu molar ratio as that of Ni_2Cu_1 (Table 1, entry 15), in comparison to the Ni_2Cu_1 catalyst. The aforementioned results verify that both the synergy between Ni-Cu in the alloy structure and strong metal-support interactions should play important roles in improving catalytic dehydrogenation-hydrogenation performance of catalysts.

Table 1 Catalytic performance of various catalysts in the coupling process between the dehydrogenation of CHL and the hydrogenation of HMF. [a]

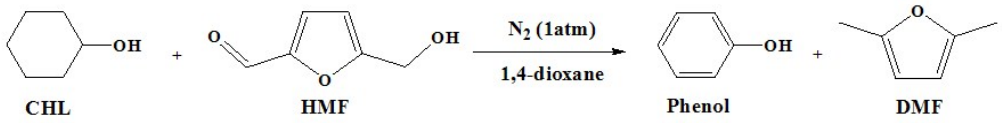

Entry	Catalyst	Temp. (°C)	Con.% (CHL)	Con.% (HMF)	Selectivity (%) [b]			Selectivity (%) [c]		
					Phenol	CHN	CHO	DMF	MFA	DMTHF
1	Ni_3Cu_0	200	99	99	36	45	18	95	0	5
2	Ni_2Cu_1	200	98	99	42	47	10	96	3	0
3	$Ni_{1.5}Cu_{1.5}$	200	83	97	26	54	19	88	12	0
4	Ni_1Cu_2	200	71	93	10	83	5	67	32	0
5 [d]	Ni_0Cu_3	200	65	90	0	99	0	40	51(9)	0
6	Ni_3Cu_0	240	99	99	78	16	6	83	0	17
7	Ni_2Cu_1	240	99	99	98	2	0	99	0	0
8	$Ni_{1.5}Cu_{1.5}$	240	94	99	46	42	11	96	3	0
9	Ni_1Cu_2	240	87	99	23	62	14	92	8	0
10	Ni_0Cu_3	240	82	99	10	85	3	77	23	0
11 [e]	Ni_2Cu_1	240	76	89	88	12	0	90	10	0
12	Ni/Al_2O_3	240	70	87	52	43	5	85	15	0
13 [d]	Cu/Al_2O_3	240	62	76	0	99	0	59	23(18)	0
14	$Ni\text{-}Cu/Al_2O_3$	240	72	91	58	35	7	89	11	0
15 [f]	Ni_3Cu_0+Ni_0Cu_3	240	95	99	37	58	5	81	19	0

[a] Reaction conditions: N_2: 1 atm, CHL/HMF = 2 (in mole), N_2/(CHL + HMF) = 13 (in mole), LHSV(CHL + HMF) = 1.0 h^{-1}. [b] Isolated selectivity of the dehydrogenation part. [c] Isolated selectivity of the hydrogenation part. [d] The numbers in parentheses refer to the selectivity of 2,5-dihydroxymethylfuran (DHMF). [e] No solvents, LHSV(CHL + HMF) = 0.5 h^{-1}. [f] The physical mixture of Ni_3Cu_0 and Ni_0Cu_3 catalysts.

The coupling process was performed over the Ni_2Cu_1 catalyst at different temperatures and liquid hourly space velocity (LHSV) values to investigate the product distributions. As shown in Fig. 3a and 3b, the conversions of CHL and HMF increase with the increasing reaction temperature. When the reaction temperature is above 200 °C, almost complete conversions are achieved. However, the selectivities to phenol and DMF vary substantially with the reaction temperature. For the CHL dehydrogenation (Fig. 3a), the main dehydrogenation product is CHN at lower reaction temperatures (< 220 °C), in addition to phenol and cyclohexen-1-one (CHO). With the reaction temperature raised up to 260 °C, the phenol selectivity reaches about 100%. Meantime, for the HMF hydrogenation part (Fig. 3b), low reaction temperatures (< 220 °C) results in the formation of a small amount of 5-methyl-2-furanmethanol (MFA) hydrogenation intermediate, besides DMF. At 240 °C, a highest DMF selectivity of 99% is achieved. As the reaction temperature is further raised to 260 °C, a certain amount of DMTHF is formed due to the deep hydrogenation of the furan ring in DMF, thus causing a slight decrease in the DMF yield.

View Article Online
DOI: 10.1039/C7GC01387F

Fig. 3c and 3d depicts the dependence of product distributions on LHSV values applied in the coupling process. It is noted that the total yields of both dehydrogenation products and hydrogenation products are low when the LHSV is below 0.6 h^{-1}, due to the easy occurrence of the condensation between CHL and HMF or between the intermediates in a long residence time. Moreover, a small amount of DMTHF is produced at low LHSV values (< 1.0 h^{-1}). As the LHSV increases from 1.0 h^{-1} to 1.6 h^{-1}, the conversions of CHL and HMF, as well as the selectivities to phenol and DMF, decrease gradually, and the yields of CHN, CHO, and MFA increase remarkably. An appropriate LHSV value of 1.0 h^{-1} benefits the production of phenol with high yield, accompanied by the disappearance of CHN and CHO dehydrogenation products. The above results verify that phenol can be formed through the dehydrogenations taking CHN and CHO as intermediates.

On the other side, as shown in scheme S1†, single CHL dehydrogenation to phenol is an endothermic process (+189.8 kJ mol^{-1}), whereas single HMF hydrogenation to DMF is exothermic by about -277.5 kJ mol^{-1}. Clearly, the coupling process combines dehydrogenation and hydrogenation into one catalytic system, thus leading to a highly effective usage of hydrogen through hydrogen transfer between two substrates, as well as a better thermal balance with a lower heat release (-87.7 kJ mol^{-1}).Therefore, much easier temperature control can be achieved in the practical operation.[18]

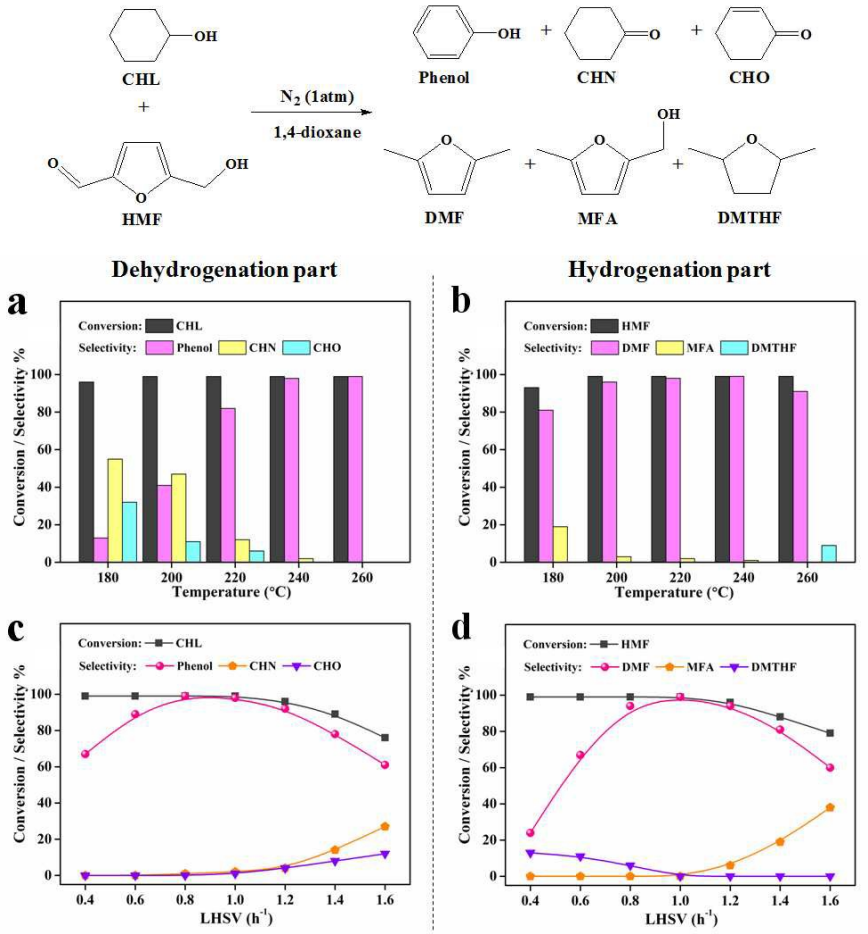

Fig. 3 Change in the conversions and selectivies over Ni_2Cu_1 catalyst in the coupling process with the reaction temperature and LHSV in the CHL dehydrogenation part (a and c) and in the HMF hydrogenation part (b and d). Reaction conditions: N_2: 1 atm, CHL/HMF = 2 (in mole), N_2/(CHL + HMF) = 13 (in mole), LHSV(CHL + HMF) = 1.0 h^{-1} (for a and b), T = 240 °C (for c and d).

View Article Online
DOI: 10.1039/C7GC01387F

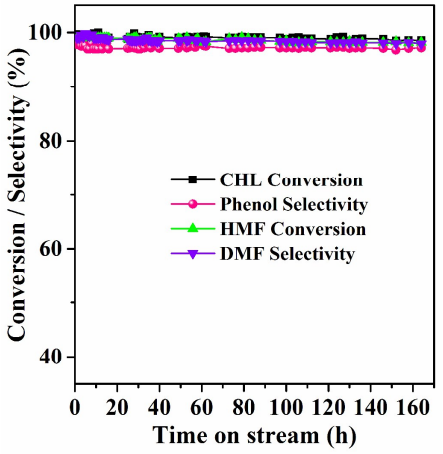

Fig. 4 Conversions and selectivities as function of time on stream over the Ni_2Cu_1catalyst. Reaction conditions: N_2: 1 atm, CHL/HMF = 2 (in mole), N_2/(CHL + HMF) = 13 (in mole), LHSV(CHL + HMF) = 1.0 h^{-1}, T = 240 °C.

Fig. 4 shows the conversions of CHL and HMF and the selectivities to phenol and DMF as functions of time on stream over the Ni_2Cu_1 catalyst. During the 160 h continuous test, no obvious decline in both the conversions and the selectivities is observed, mirroring its excellent structural stability. The turnover number (TON) values, which were calculated based on the moles converted CHL or HMF per mole of Ni and Cu in the catalyst, are about 77.9 for CHL and 48.6 for HMF, respectively. ICP-AES measurements reveal that the decrease in total content of Ni and Cu in the catalyst is less than 0.4 wt.% after reaction, indicating that there is a slight leaching of the active composition in the catalyst during the reaction. Therefore, the stability of the catalyst needs to be further improved. The related investigations will be made in the future. The above results further confirm the advantage for the present bimetallic Ni-Cu alloy catalyzed dehydrogenation-hydrogenation coupling process for the production of phenol and DMF.

Reaction pathways and mechanism

As we know, the HMF hydrogenation under H_2 atmosphere mainly involves the hydrogenation of C=O bond and the hydrogenolysis of C–O bond.[6,7] Previously, in most cases, CHN was reported to be the main dehydrogenation product using CHL as hydrogen donator in transfer hydrogenations. To date, the production of phenol by oxygen-free dehydrogenation of CHL coupled with the HMF hydrogenation has not been

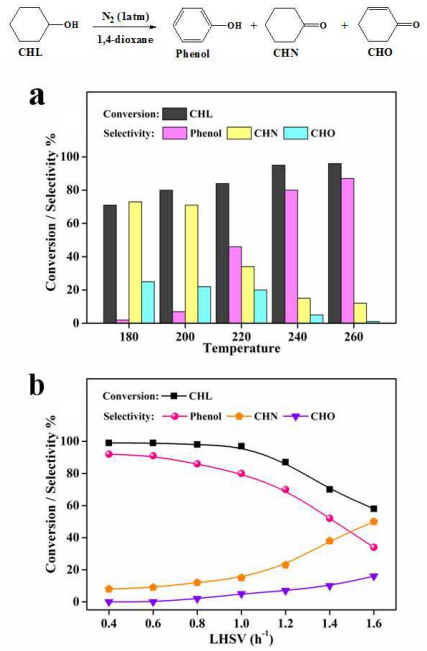

Fig. 5 Change in the conversions and selectivities over Ni_2Cu_1 catalyst with the reaction temperature (a) and the LHSV value (b) in the CHL dehydrogenation. Reaction conditions: N_2: 1 atm, N_2/CHL = 13 (in mole), LHSV(CHL) = 1.0 h^{-1} (for a), T = 240 °C (for b).

studied. In order to deeply investigate the reaction pathways in the present coupling process, the following control experiments were conducted over the Ni_2Cu_1 catalyst.

Firstly, the CHL dehydrogenation was carried out in the absence of HMF under N_2 atmosphere, ruling out the possible role of HMF. The reaction results are displayed in Fig. 5. Notably, the CHL conversions are significantly restrained at the same temperatures as those in the coupling process (Fig. 5a). In this case, the absence of hydrogen acceptor (HMF), however, leads to decreased phenol selectivities at different reaction temperatures, compared with those in the coupling process. In addition, it is noted from Fig. 5b that the phenol selectivity declines rapidly with the increasing LHSV value, whereas CHN increases remarkably in yield and becomes the main product at a high LHSV value of 1.6 h^{-1}. It suggests that the CHL dehydrogenation can be substantially promoted by coupling with the HMF hydrogenation, and HMF as hydrogen acceptor drives the reaction equilibrium of the CHL dehydrogenation toward the generation of phenol in the coupling process.

Secondly, to verify the crucial role of the dehydrogenation playing in the HMF hydrogenation, CHN and CHO were employed as substrates to substitute CHL in different dehydrogenation-hydrogenation coupling processes over the Ni_2Cu_1 catalyst (Fig. 6). Noticeably, the CHN dehydrogenation produces both phenol in high yields and CHO in low yields even at relatively high LHSV values. In the meantime, the DMF selectivities (LHSV > 0.8 h^{-1}) are lower than those in the

View Article Online
DOI: 10.1039/C7GC01387F

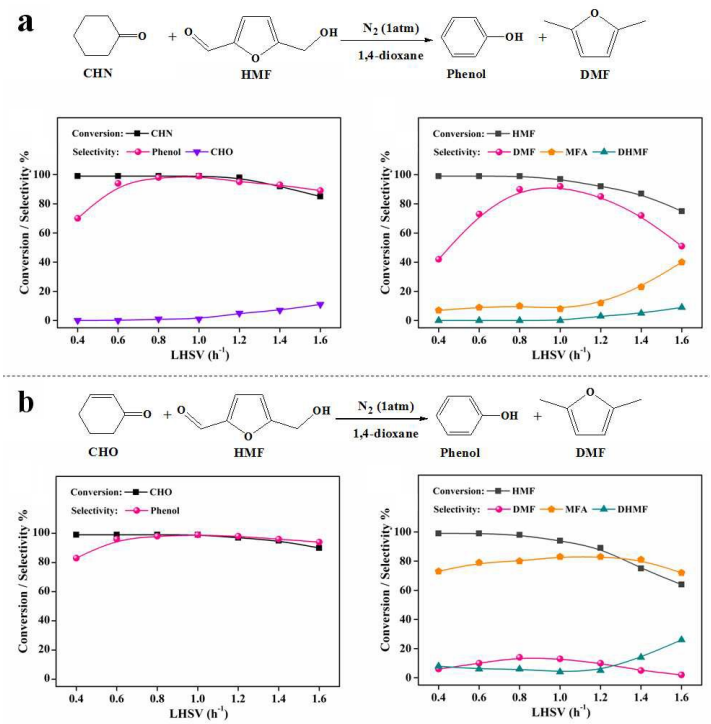

Fig. 6 Change in the conversions and selectivities over Ni_2Cu_1 catalyst with the LHSV value in the coupling process starting from (a) CHN and HMF and (b) CHO and HMF. Reaction conditions: N_2: 1 atm, CHN/HMF = 2 (in mole), CHO/HMF = 2 (in mole), N_2/(CHN + HMF) = 13 (in mole), N_2/(CHO + HMF) = 13 (in mole), T = 240 °C.

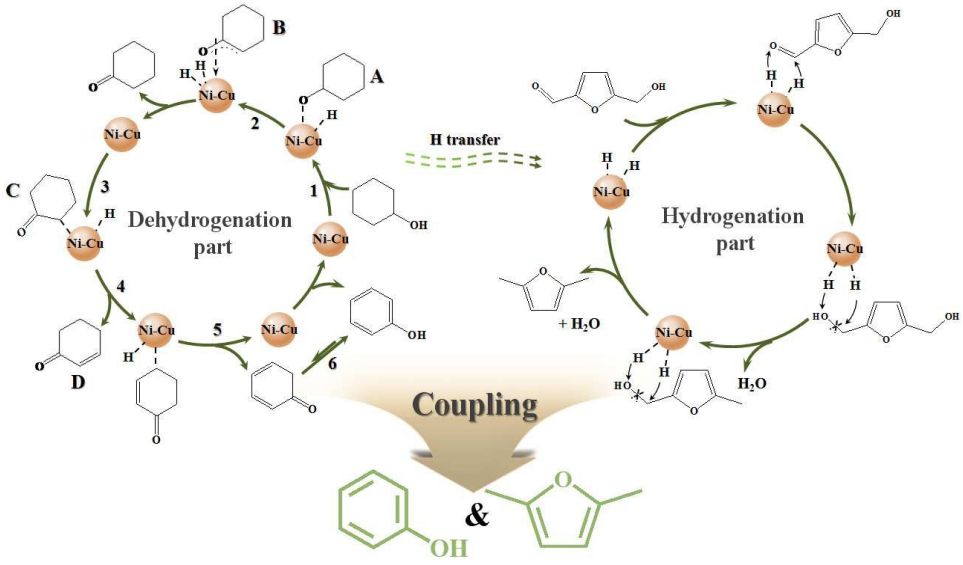

Scheme 2 Plausible reaction pathways for the coupling process between the CHL dehydrogenation and the HMF hydrogenation over as-formed Ni_xCu_y catalysts.

case of coupling process starting from CHL and HMF. And accordingly, the yields of MFA and 2,5-dihydroxymethylfuran (DHMF) are enhanced quickly with the increasing LHSV value at the expense of the DMF selectivity at higher LHSV values, due to the lack of active hydrogen species produced from the CHN dehydrogenation. For the coupling process starting from CHO and HMF, phenol is the only dehydrogenated product and almost complete conversion of CHO to phenol occurs at the LHSV value of 0.8 h^{-1}; while MFA is a major hydrogenation product together with DHMF. Therefore, positive correlations can be established between the amount of the *in-situ* generated active hydrogen species and the DMF selectivity in the HMF

View Article Online
DOI: 10.1039/C7GC01387F

hydrogenation, implying that an appropriate substrate should be critical for the present coupling process producing phenol and HMF with high yields. The above observations clearly reflect three tandem steps for the conversion of CHL through CHL to CHN, CHN to CHO, and CHO to phenol in the coupling process starting from CHL and HMF, and HMF is concurrently hydrogenated to DMF using active hydrogen species released from the dehydrogenations of CHL, CHN, or CHO.

At last, the dehydrogenation-hydrogenation coupling process starting from CHN and HMF was also conducted over different catalysts. As shown in Table S2†, Ni_2Cu_1 catalyst exhibits the best dehydrogenation and hydrogenation performances among all Ni_xCu_y catalysts. In contrast, much lower conversions of CHN and HMF are observed over the Ni_0Cu_3. In addition, Al_2O_3-supported monometallic and bimetallic comparison samples show poorer catalytic dehydrogenation and hydrogenation activities, in comparison to their corresponding Ni_xCu_y catalysts. The above results further confirm that the dehydro-aromatization and hydrogenation abilities of Ni species are much stronger than those of Cu species, and that the nanostructure of bimetallic Ni-Cu alloy plays a crucial role in promoting the dehydrogenation-hydrogenation coupling process.

In view of the above catalytic reaction results, a plausible mechanism for the dehydrogenation–hydrogenation coupling process through the hydrogen transfer between CHL and HMF over as-formed Ni_xCu_y catalysts is proposed tentatively at a molecular level (Scheme 2). For the CHL dehydrogenation, firstly, the hydroxyl group in CHL interacts with active metallic sites on the catalyst, and the hydrogen atom is abstracted to form the metal alkoxide species (R–O–M) (step **1**, compound **A**). Then, the catalyst capture another β-H atom adjacent to the alcoholic group to form the π-allylic species (step **2**, compound **B**), which may exist as a transitional structure between ketone and enol and then give CHN and active hydrogen species. Sequentially, the adsorbed CHN suffers a α-C–H activation process and coordinates with the catalyst to form the metal enolate species (step **3**, compound **C**), then the β-H elimination proceeds again to give the second intermediate CHO (step **4**, compound **D**). At last, the dehydrogenation of CHO, which takes place through a similar process to that of CHN (step **5**), and tautomeric transformation of CHO lead to the formation of final phenol product (step **6**). During the whole dehydrogenation process of CHL and intermediates, active hydrogen species are continuously abstracted to take part in the HMF hydrogenation for the production of DMF.

One fact should be underlined that Ni-rich catalysts possesses high dehydrogenation activity and are highly selective to phenol even under relatively low reaction temperatures, which should be correlated with the intrinsic high aromatization activity of nickel.[19] Correspondingly, the dehydrogenation of ring easily occurs through the formation of metal-carbon bonds with σ- or π-type character on such a kind of "aromatizing metal". Another phenomenon is that the introduction of an appropriate amount of Cu into Ni-Cu alloy system can enhance the yields of phenol and DMF. This may be reasonably related to the synergistic effect of Ni-Cu alloy nanostructure. In order to get an insightful understanding of the synergy between Ni-Cu species in reduced catalysts, X-ray photoelectron spectroscopy (XPS) characterizations of the catalysts were performed (Fig. 7). Obviously, the values of binding energy (BE) of Ni $2p_{3/2}$ core level in bimetallic Ni-Cu catalysts are lower than that in the monometallic Ni one. Intriguingly, the change in the BE values of Cu $2p_{3/2}$ core level in catalysts exhibit an opposite trend. This phenomenon suggests the presence of electron transfer from Cu to Ni in the alloy structure, thanks to the electronic (ligand) effect. Such electronic effect would benefit the β-hydride elimination, thereby promoting the dehydrogenation reaction.[12c,20] Therefore, manipulating the Ni/Cu molar ratio in catalysts is capable of concurrently improving the yields of phenol and DMF products in the present coupling process, which has never been reported before. Nevertheless, how metallic sites in bimetallic Ni-Cu alloy structure cooperate in the present coupling process catalysis to dictate the high selectivities to phenol and DMF still need to be further systemically investigated.

For the HMF hydrogenation, a commonly accepted reaction path is that HMF is firstly converted to DHMF or MFA and further to DMF.[6,7] This is also supported by the single HMF hydrogenation using external H_2 (Fig. S3†). One can found that the content of MFA intermediate is remarkably increased with the increasing LHSV value from 1.0 to 1.8 h^{-1}, similar to that in the case of the coupling process. As described above, however, the product distributions in the HMF hydrogenation is closely related to the amount of released active hydrogen species in the coupling process without external hydrogen. When CHL is converted to phenol with high yields, the amount of *in situ* produced hydrogen species is sufficient for the HMF hydrogenation to form DMF. However, if CHL is incompletely converted or partial dehydrogenated to CHN, high yields of hydrogenation intermediates (e.g. DHMF or MFA) can be formed. On the other hand, the high activity of metallic Ni puts forward the possibility of the deep hydrogenation of furan ring to give DMTHF, thus decreasing the DMF yield. On the

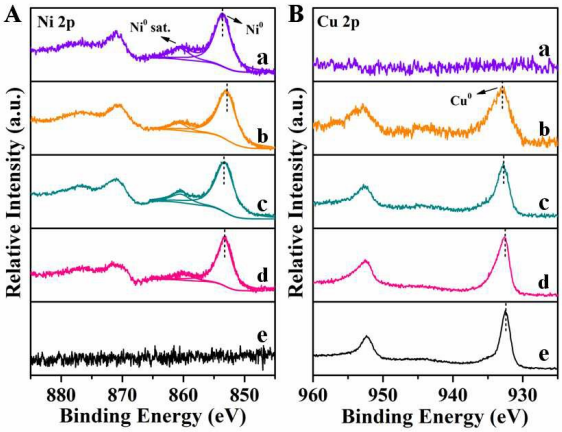

Fig. 7 Ni 2p XPS (A) and Cu 2p XPS (B) of Ni_xCu_y catalysts. (a) Ni_3Cu_0, (b) Ni_2Cu_1, (c) $Ni_{1.5}Cu_{1.5}$, (d) Ni_1Cu_2, (e) Ni_0Cu_3.

View Article Online
DOI: 10.1039/C7GC01387F

contrary, due to the overlapping of the 3d band of Cu atoms and the anti-bonding orbital of furan ring,[8d,21] Cu-contained samples usually strongly repulses the furan ring. Consequently, the C–OH bond can be preferentially dissociated rather than the C–C one. As a result, the aromatic hydrogenation is minimized and high yields of DMF can be gained over bimetallic Ni-Cu alloy catalysts.

Table 2 Catalytic reaction results over the Ni_2Cu_1 catalyst in the dehydrogenation-hydrogenation coupling processes between substituted CHLs and HMF. [a]

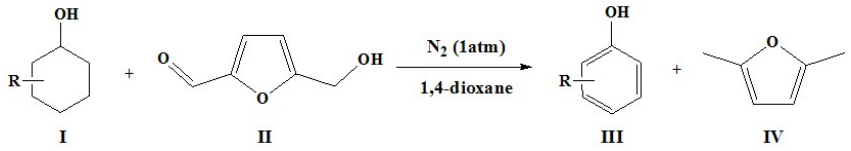

I II III IV

Entry	Substrate (I)	Temp. (°C)	LHSV (h^{-1})	Yield % (III) [b]	Yield % (IV) [c]
1	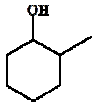	240	1.0	79	98
2	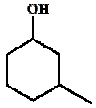	240	1.0	87	99
3	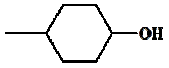	240	1.0	92	99
4	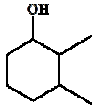	250	0.8	78	98
5	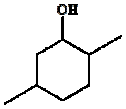	250	0.8	76	95
6	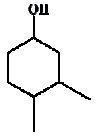	250	1.0	89	99
7	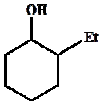	240	1.0	72	94
8	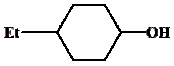	240	1.0	85	98
9	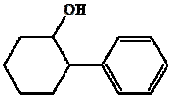	250	0.8	88	99

[a] Reaction conditions: N_2: 1 atm, I/II = 2 (in mole), N_2/(I + II) = 13 (in mole), LHSV(I + II) = 1.0 h^{-1}. [b] Isolated yield of the dehydrogenation part. [c] Isolated yield of the hydrogenation part.

The feasibility of Ni_xCu_y catalyst for the coupling process

The present dehydrogenation-hydrogenation coupling protocol was further extended to produce various substituted phenols and DMF to verify the scope, activity, and chemoselectivity of the Ni_2Cu_1 catalyst (Table 2). Notably, the Ni_2Cu_1 catalyst also

View Article Online
DOI: 10.1039/C7GC01387F

exhibited good catalytic activity and chemoselectivity for the dehydrogenation of various substituted CHLs and the hydrogenation of HMF, with high yields of substituted phenols and DMF. Compared with those for monomethyl-substituted CHLs (entries 1-3), dehydrogenation-aromatization activities for dimethyl-substituted CHLs (entries 4-6) are lower due to the steric effect, along with higher reaction temperatures and (or) lower LHSV values required. Furthermore, selective dehydrogenations of substituted ethyl- and phenyl CHLs can successfully proceed (entries 7-9). Meanwhile, the DMF selectivities maintain above 94 % in all cases. The above results clearly verify the extensive applicability of the present coupling process between the dehydrogenation of substituted CHLs and the hydrogenation of HMF for the highly efficient synchronized production of DMF and various substituted phenols.

Conclusions

In summary, we developed a highly efficient vapor-phase coupling process between the CHL dehydrogenation and the HMF hydrogenation to simultaneously produce phenol and DMF with high yields (> 97%), over the noble metal-free Ni-Cu alloy nanocatalyst with the Ni/Cu molar ratio of 2:1 in the absence of any external hydrogen and oxygen supply. Systematic catalytic tests revealed that CHL could be dehydrogenated into phenol *via* CHN and CHO intermediates. Meanwhile, *in situ* produced active hydrogen species from the dehydrogenation of CHL, CHN, or CHO could react with HMF to generate DMF. Furthermore, HMF as hydrogen acceptor derived the reaction equilibrium of the CHL dehydrogenation toward the generation of phenol in the coupling process. It was found that the Ni-Cu alloy nanostructure substantially facilitated the coupling process along with high yields of both phenol and DMF, due to the fact that the electronic effect in the Ni-Cu alloy structure benefited the β-hydride elimination in the dehydrogenation and effectively restrained the aromatic hydrogenation. Besides, a variety of substituted phenols also could be produced through the present coupling system. As-developed coupling process provides a promising and simple avenue for the green production of industrial chemicals and biofuels from fundamental raw materials, which highlights the idea of green chemistry and sustainable development greatly.

Conflicts of interest

There are no conflicts of interest to declare.

Acknowledgements

This study was funded through National Natural Science Foundation of China (21325624; 21521005) and Fundamental Research Funds for the Central Universities (buctrc201528).

Notes and references

1 a) J. N. Chheda, G. W. Huber and J. A. Dumesic, *Angew. Chem. Int. Ed.*, 2007, **46**, 7164–7183; b) P. P. Upare, D. W. Hwang, Y. K. Hwang, U. -H. Lee, D. -Y. Hong and J. -S. Chang, *Green Chem.*, 2015, **17**, 3310–3313.

2 a) R. -J. van Putten, J. C. van der Waal, E. de Jong, C. B. Rasrendra, H. J. Heeres and J. G. de Vries, *Chem. Rev.*, 2013, **113**, 1499–1597; b) J.C. Colmenares and R. Luque, *Chem. Soc. Rev.*, 2014, **43**, 765–778.

3 a) Y. Román-Leshkov, C. J. Barrett, Z. Y. Liu and J. A. Dumesic, *Nature*, 2007, **447**, 982–985; b) J. -P. Lange, R. Price, P. M. Ayoub, J. Louis, L. Petrus, L. Clarke and H. Gosselink, *Angew. Chem. Int. Ed.*, 2010, **49**, 4479–4483.

4 a) M. J. Climent, A. Corma and S. Iborra, *Green Chem.*, 2014, **16**, 516–547; b) B. Zhou, J. Song, H. Zhou, T. Wu and B. Han, *Chem. Sci.*, 2016, **7**, 463–468; c) F. M. A. Geilen, B. Engendahl, A. Harwardt, W. Marquardt, J. Klankermayer and W. Leitner, *Angew. Chem. Int. Ed.*, 2010, **49**, 5510–5514.

5 a) J. J. Bozell and G. R. Petersen, *Green Chem.*, 2010, **12**, 539–554; b) S. P. Teong, G. Yi and Y. Zhang, *Green Chem.*, 2014, **16**, 2015–2026; c) M. E. Zakrzewska, E. Bogel-Łukasik and R. Bogel-Łukasik, *Chem. Rev.*, 2011, **111**, 397–417; d) M. J. Climent, A. Corma and S. Iborra, *Green Chem.*, 2011, **13**, 520–540; e) A. A. Rosatella, S. P. Simeonov, R. F. M. Fraude and C. A. M. Afonso, *Green Chem.*, 2011, **13**, 754–793; f) Y. Nakagawa, M. Tamura, K. Tomishige, *ACS Catal.*, 2013, **3**, 2655–2668; g) J. Mitra, X. Zhou and T. Rauchfuss, *Green Chem.*, 2015, **17**, 307–313; h) A. S. K. Hashmi, M. Wölfle, J. H. Teles and W. Frey, *Synlett*, 2007, **11**, 1747–1752; i) S. Tšupova, F. Rominger, M. Rudolph and A. S. K. Hashmi, *Green Chem.*, 2016, **18**, 5800–5805; j) A. S. K. Hashmi, T. M. Frost and J. W. Bats, *J. Am. Chem. Soc.*, 2000, **122**, 11553–11554; k) T. Buntara, S. Noel, P. H. Phua, I. Melián-Cabrera, J. G. de Vries and H. J. Heeres, *Angew. Chem. Int. Ed.*, 2011, **50**, 7083–7087; l) M. J. Gilkey and B. Xu, *ACS Catal.*, 2016, **6**, 1420–1436; m) A. S. K. Hashmi, P. Haufe, C. Schmid, A. R. Nass and W. Frey, *Chem. Eur. J.*, 2006, **12**, 5376–5382.

6 a) M. Chidambaram and A. T. Bell, *Green Chem.*, 2010, **12**, 1253–1262; b) J. Jae, W. Q. Zheng, A. M. Karim, W. Guo, R. F. Lobo and D. G. Vlachos, *ChemCatChem*, 2014, **6**, 848–856; c) J. B. Binder and R. T. Raines, *J. Am. Chem. Soc.*, 2009, **131**, 1979–1985; d) J. Jae, W. Zheng, R. F. Lobo and D. G. Vlachos, *ChemSusChem*, 2013, **6**, 1158–1162.

7 a) G. H. Wang, J. Hilgert, F. H. Richter, F. Wang, H. J. Bongard, B. Spliethoff, C. Weidenthaler and F. Schuth, *Nat. Mater.*, 2014, **13**, 293–300; b) M. Chatterjee, T. Ishizaka and H. Kawanami, *Green Chem.*, 2014, **16**, 1543–1551; c) M. Y. Chen, C. B. Chen, B. Zada and Y. Fu, *Green Chem.*, 2016, **18**, 3858–3866; d) Y. B. Huang, M. Y. Chen, L. Yan, Q. X. Guo and Y. Fu, *ChemSusChem*, 2014, **7**, 1068–1072; e) Y. H. Zu, P. P. Yang, J. J. Wang, X. H. Liu, J. W. Ren, G. Z. Lu and Y. Q. Wang, *Appl. Catal., B*, 2014, **146**, 244–248; f) J. Luo, H. Yun, A. V. Mironenko, K. Goulas, J. D. Lee, M. Monai, C. Wang, V. Vorotnikov, C. B. Murray, D. G. Vlachos, P. Fornasiero and R. J. Gorte, *ACS Catal.*, 2016, **6**,

View Article Online
DOI: 10.1039/C7GC01387F

4095-4104; g) G.-H. Wang, J. Hilgert, F. H. Richter, F. Wang, H.-J. Bongard, B. Spliethoff, C. Weidenthaler and F. Schüth, *Nat. Mater.*, 2014, **13**, 293–300; h) J. Luo, L. Arroyo-Ramírez, J. Wei, H. Yun, C. B. Murray and R. J. Gorte, *Appl. Catal., A*, 2015, **508**, 86–93.

8 a) T. S. Hansen, K. Barta, P. T. Anastas, P. C. Ford and A. Riisager, *Green Chem.*, 2012, **14**, 2457–2461; b) T. Thananatthanachon and T. B. Rauchfuss, *Angew. Chem., Int. Ed.*, 2010, **49**, 6616–6168; c) S. De, S. Dutta and B. Saha, *ChemSusChem*, 2012, **5**, 1826–1833; d) D. Scholz, C. Aellig and I. Hermans, *ChemSusChem*, 2013, **7**, 268–275; e) T. Pasin, A. Lolli, S. Albonetti, F. Cavani and M. Mella, *J. Catal.*, 2014, **317**, 206–219; f) A. M. Ruppert, M. Jędrzejczyk, O. Sneka-Płatek, N. Keller, A. S. Dumon, C. Michel, P. Sautet and J. Grams, *Green Chem.*, 2016, **18**, 2014–2028.

9 Z. Rappoport, *The Chemistry of Phenols*, Wiley-VCH, New York, 2003.

10 a) C. Hoarau and T. R. R. Pettus, *Synlett*, 2003, **1**, 127–137; b) P. Hanson, J. R. Jones, A. B. Taylor, P. H. Walton and A. W. Timms, *J. Chem. Soc., Perkin Trans.,* 2002, **6**, 1135–1150; c) J. Zhang, Q. Jiang, D. Yang, X. Zhao, Y. Dong and R. Liu, *Chem. Sci.*, 2015, **6**, 4674–4680.

11 R. Kumar, S. Sithambaram and S.L. Suib, *J.Catal.,* 2009, **262**, 304-313.

12 a) Y. Izawa, D. Pun and S. S. Stahl, *Science*, 2011, **333**, 209–213; b) Y. Izawa, C. Zheng and S. S. Stahl, *Angew. Chem., Int. Ed.*, 2013, **52**, 3672–3675; c) D. Pun, T. Diao and S. S. Stahl, *J. Am. Chem. Soc.*, 2013, **135**, 8213–8221; d) X. Jin, K. Taniguchi, K. Yamaguchi and N. Mizuno, *Chem. Sci.*, 2016, **7**, 5371–5383; e) T. Moriuchi, K. Kikushima, T. Kajikawa and T. Hirao, *Tetrahedron Lett.*, 2009, **50**, 7385–7387; f) J. Muzart, *Eur. J. Org. Chem.*, 2010, **2010**, 3779–3790.

13 a) Q. Hu, G. Fan, L. Yang, X. Cao, P. Zhang, B. Wang and F. Li, *Green Chem.*, 2016, **18**, 2317–2322; b) Q. Yang, Y. Z. Chen, Z. U. Wang, Q. Xu and H. L. Jiang, *Chem. Commun.*, 2015, **51**, 10419–10422; c) Y. L. Zhu, H. W. Xiang, G. S. Wu, L. Bai and Y. W. Li, *Chem. Commun.*, 2002, **3**, 254–255; d) Y. L. Zhu, J. Yang, G. Q. Dong, H. Y. Zheng, H. H. Zhang, H. W. Xiang and Y. W. Li, *Appl. Catal., B*, 2005, **57**, 183–190; e) J. Song, L. Wu, B. Zhou, H. Zhou, H. Fan, Y. Yang, Q. Meng and B. Han, *Green Chem.*, 2015, **17**, 1626–1632.

14 a) H. P. R. Kannapu, C. K. P. Neeli, K. S. R. Rao, V. N. Kalevaru, A. Martin and D. R. Burri, *Catal. Sci. Technol.*, 2016, **6**, 5494–5503; b) H. Y. Zheng, Y. L. Zhu, L. Huang, Z. Y. Zeng, H. J. Wan and Y. W. Li, *Catal. Commun.*, 2008, **9**, 342–348.

15 a) H. Y. Zheng, Y. L. Zhu, Z. Q. Bai, L. Huang, H. W. Xiang and Y. W. Li, *Green Chem.*, 2006, **8**, 107–109; b) B. M. Nagaraja, A. H. Padmasri, P. Seetharamulu, K. H. P. Reddy, B. D. Raju and K. S. R. Rao, *J. Mol. Catal.*, 2007, **278**, 29–37.

16 a) G. Fan, F. Li, D. G. Evans and X. Duan, *Chem. Soc. Rev.*, 2014, **43**, 7040–7066; b) F. Li and X. Duan, *Struct. Bonding*, 2006, **119**, 193–223.

17 a) J. G. Dickinson and P. E. Savage, *ACS Catal.*, 2014, **4**, 2605–2615; b) E. T. Saw, U. Oemar, X. R. Tan, Y. Du, A. Borgna, K. Hidajat and S. Kawi, *J. Catal.*, 2014, **314**, 32–46; c) A. Ungureanu, B. Dragoi, A. Chirieac, S. Royer, D. Duprez and E. Dumitriu, *J. Mater. Chem.*, 2011, **21**, 12529–12541.

18 a) Y. Zhu, H. Xiang, G. Wu, L. Bai and Y. Li, *Chem. Commun.*, 2002, 254–255; b) Y. Zhu, H. Xiang, Y. Li,*a H. Jiao, G. Wu, B. Zhong and G. Guo, *New J. Chem.*, 2003, **27**, 208–210.

19 M. Dobrovolszky, P. Tétényi and Z. Paál, *J. Catal.*, 1982, **74**, 31–43.

20 a) A. Wang, X. Y. Liu, C. -Y. Mou and T. Zhang, *J. Catal.*, 2013, **308**, 258–271; b) J. K. Edwards, S. J. Freakley, A. F. Carley, C. J. Kiely and G. J. Hutchings, *Acc. Chem. Res.*, 2014, **47**, 845–854; c) G. J. Hutchings and C. J. Kiely, *Acc. Chem. Res.*, 2013, **46**, 1759–1772; d) H. Zhang and N. Toshima, *Catal. Sci. Technol.*, 2013, **3**, 268–278.

21 a) K. L. Deutsch and B. H. Shanks, *J. Catal.*, 2012, **285**, 235–241; b) S. Sitthisa, T. Sooknoi, Y. Ma, P. B. Balbuena and D. E. Resasco, *J. Catal.*, 2011, **277**, 1–13; c) S. Sitthisa and D. E. Resasco, *Catal. Lett.*, 2011, **141**, 784–791; d) Y. S. Yun, D. S. Park and J. Yi, *Catal. Sci. Technol.*, 2014, **4**, 3191–3202; e) T. Wang, M. W. Nolte and B. H. Shanks, *Green Chem.,* 2014, **16**, 548–572.

View Article Online
DOI: 10.1039/C7GC01387F

A table of contents entry

Highly efficient synchronized production of phenol and 2,5-dimethylfuran was achieved via a bimetallic Ni-Cu catalyzed dehydrogenation-hydrogenation coupling process.